Discrete breathers in crystals with NaCl structure

Liya Z. Khadeeva and Sergey V. Dmitriev
Institute for Metals Superplasticity Problems, Russian Academy of Science, Khalturin Street 39, Ufa 450001, Russia
(Received 10 March 2010; revised manuscript received 12 May 2010; published 29 June 2010)

Molecular-dynamics method is used to study the influence of mass ratio of anions and cations on the phonon spectrum of the crystal with NaCl structure and on the conditions of existence and properties of gap discrete breathers (DBs). We show that DBs can be easily excited when the mass ratio of light to heavy components is less than 0.2 and the gap in the phonon spectrum is sufficiently wide. Nonexistence of DBs for larger mass ratios is explained through the excitation of the harmonic with the frequency equal to half of the main DB frequency that interacts with phonons below the gap. For the mass ratio equal to 0.1 we could find at least three types of stable DBs that differ by the number of atoms with the largest amplitude and by polarization of oscillations. A zone-boundary phonon mode with sufficiently large amplitude was found to be modulationally unstable. Dynamics of such mode lead to spontaneous localization of energy in the form of large-amplitude DBs according to the anti-Fermi-Pasta-Ulam mechanism.

DOI: 10.1103/PhysRevB.81.214306 PACS number(s): 05.45.Yv, 63.20.−e

I. INTRODUCTION

Intrinsic localized modes or discrete breathers (DBs) are the spatially localized vibrational modes of large amplitude in nonlinear defect-free lattices whose existence was proved theoretically.[1] The role of DBs has being extensively discussed during the past two decades in relation to many physical systems ranging from the chains of superconducting Josephson junctions and DNA models to the nonlinear optical waveguide arrays and Bose-Einstein condensate, as described in the recent reviews.[2–5]

Over the past few years, there has been increasing interest in the study of DBs in the solid state physics[6–12] and materials science.[13–15] Manley *et al.*[6] have reported on the experimental observation of gap DBs in thermodynamic equilibrium in NaI crystal, in line with the molecular dynamics simulation results published earlier by Kiselev and Sievers.[7] In their recent work,[8] Bishop *et al.* have discussed the relaxor behavior of ferroelectric perovskite oxides taking into account their inherent anharmonicity and the possibility to support DBs. DBs exist in carbon nanotubes and they play important role in the structure reconstruction of nanotubes under axial tension.[16,17] Molecular-dynamics simulations by Savin and Kivshar have demonstrated that armchair graphene nanoribbons can support vibrational localized states in the form of surface solitons and breathers.[9] The anti-Fermi-Pasta-Ulam (anti-FPU) mechanism of energy localization[18] was studied in the one- and two-dimensional diatomic lattices supporting gap DBs.[10–12] The void ordering, observed in a number of metals and alloys under neutron and heavy-ion irradiations was shown to be possible through the excitation of DBs.[13] Manley[14,15] has discussed a possible use of DBs in making a thermal rectifier and also the mechanisms how DBs modify properties of materials.

In order to preserve its identity, DB must have oscillation frequency and all its higher harmonics lying outside the phonon bands of the crystal lattice. Molecular-dynamics simulations have recently revealed that diatomic crystals with Morse interatomic interactions typically demonstrate soft type of anharmonicity.[10] In these circumstances, DB's frequency decreases with increase in its amplitude and one can expect to find only so-called gap DBs with frequency within the phonon gap of the crystal. Gap DBs in diatomic lattices of low dimensions were studied theoretically in a number of works.[19,20] A necessary condition of existence of such DBs is the presence of a sufficiently wide gap in the phonon spectrum of the crystal. Gaps in the phonon bands can be expected in crystals with components having sufficiently different atomic weights. For instance, DBs in NaI crystal are the gap DBs.[6,7] We thus come to the question how the atomic weight ratio in a family of crystals can affect the width of the phonon gap and the conditions of existence of DBs.

In this paper, by means of molecular-dynamics simulations, we study conditions of existence and properties of gap DBs in crystals with NaCl structure. Several crystals of this family are listed in Table I with the ratios of atomic weights of light to heavy components.

We also study the dynamics of the modulationally unstable Brillouin-zone-boundary mode and, for a particular polarization of such mode, demonstrate that the anti-FPU mechanism of excitation of DBs (Ref. 18) does work for the considered three-dimensional crystal with realistic interatomic interactions.

The paper is organized as follows. In Sec. II we briefly describe crystal structure and present parameters of interatomic potentials used in our simulations. Section III A contains description of phonon density of states for different atomic weight ratios; Sec. III B discusses the properties of stable DBs we could excite in the crystal; Sec. III C reports on the single degree of freedom model of DB; and in Sec. III D the anti-FPU mechanism of excitation of DBs is investigated. Section IV concludes the paper.

II. SIMULATION DETAILS

NaCl structure consists of two face-centered cubic lattices with lattice parameter a, one occupied by anions and another one by cations, displaced one with respect to another by the vector $(a/2,0,0)$ so that one falls in the body centered position of the other. Each atom has six neighbors of the oppo-

TABLE I. Ratios of atomic weights of light to heavy components in some crystals with NaCl structure.

	Anion, standard atomic weight								
Cation, standard atomic weight	N, 14g/mol	O, 15.99g/mol	F, 19g/mol	S, 32.07g/mol	Cl, 35.5g/mol	Se, 78.96g/mol	Br, 80g/mol	I, 127g/mol	Te, 127.6g/mol
Li, 7g/mol			0.37		0.22		0.09	0.06	
Na, 23g/mol			0.83		0.65		0.29	0.18	
Mg, 24.3g/mol		0.66							
K, 39g/mol			0.49		0.91		0.49	0.31	
Ti, 47.87g/mol	0.29								
Rb, 85.5g/mol			0.22		0.42		0.94	0.67	
Zr, 91.2g/mol	0.15								
Ag, 107.87g/mol			0.18		0.33		0.74		
Sn, 118.7g/mol									0.93
Cs, 133g/mol			0.14		0.27		0.6	0.96	
Pb, 207.2g/mol				0.16		0.38			0.62

site type which are at the vertices of a regular octahedron. Thus, each translational cell consists of four anions and four cations as shown in Fig. 1.

Interactions between atoms are described by pairwise potentials

$$U_{KL}(r) = \frac{Q_K Q_L}{r} + f_0(b_K + b_L)\exp\left[\frac{a_K + a_L - r}{b_K + b_L}\right] - \frac{C_K C_L}{r^6}, \tag{1}$$

which consist of Coulomb interaction, Born-Mayer-type repulsion, and dispersive interaction, described by the three terms in the right-hand side of Eq. (1), respectively. Here r is the distance between atoms, $a_K(b_K)$ and $a_L(b_L)$ are the effective radiuses (softness parameters) of atoms of sort K and L with the standard force $f_0=1$ kcal Å^{-1} mol^{-1}. These or similar interatomic potentials are widely used in molecular-dynamics simulations of crystals with ionic or mixed ionic-covalent bonding.[7,21–23]

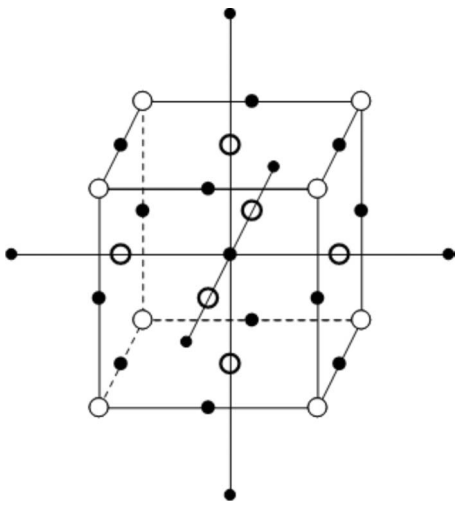

FIG. 1. The crystal with NaCl structure. Heavy (light) atoms are shown by open (filled) circles.

The main goal of our study was the investigation of the atomic weight ratio effect on the properties of DBs. That is why we took interatomic parameters that are not related to any particular crystal but give stable NaCl structure and realistic values of interaction energies, lattice parameter, vibrational frequencies, etc. Parameters of the potentials were chosen as follows: $Q_K/e=1$, $Q_L/e=-1$, where e is the absolute value of electron charge, $a_K=1.1$ Å, $a_L=2.3$ Å, $b_K=0.01$ Å, $b_L=0.1$ Å, $C_K=40.3$ kcal$^{1/2}$ Å^3 mol$^{1/2}$, and $C_L=190.0$ kcal$^{1/2}$ Å^3 mol$^{1/2}$.

For chosen parameters of potentials the equilibrium lattice parameter of the NaCl structure was found to be equal to $a=6.25$ Å. The atomic weight of the heavy atom was fixed to $M_K=100$ g/mol and for the light atom we took the values $M_L=\{10,18,20,30\}$ g/mol. This means that the following mass ratios were considered: $M_L/M_K=\{0.1,0.18,0.2,0.3\}$. Computational cell used in our simulations included up to $11\times11\times11$ translational cells and it was subjected to periodic boundary conditions.

III. NUMERICAL RESULTS

A. Phonon spectra

In Figs. 2(a)–2(c) we present the phonon density of states (DOS) of the considered three-dimensional diatomic crystal for the three different mass ratios, $M_L/M_K=0.1,0.2,0.3$. One can see that with increase in the mass ratio the width of the gap in the phonon band decreases. Gap DBs can be obtained in crystals with rather wide gap in phonon spectrum, i.e., in crystals with a small mass ratio of light to heavy atoms, M_L/M_K.

We have calculated phonon DOS for mass ratios within the range $0.1 \leq M_L/M_K \leq 1$, and in Fig. 3 we present the maximal frequency of the phonon spectrum (solid line) and the edges of the phonon gap (dashed line) as the functions of the mass ratio. One can see that, in our case, the gap is absent for $M_L/M_K > 0.7$.

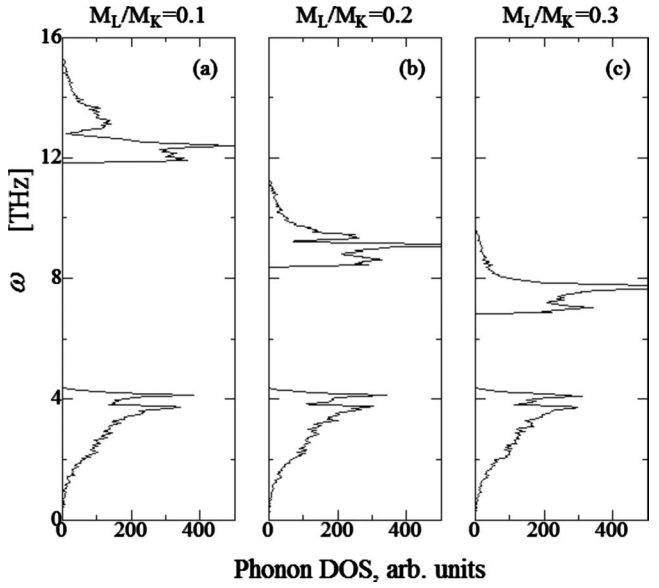

FIG. 2. Densities of states of the phonon spectra for crystals with mass ratios (a) $M_L/M_K=0.1$, (b) $M_L/M_K=0.2$, and (c) $M_L/M_K=0.3$.

B. Discrete breathers

The discrete breathers were excited simply by shifting one light atom or two neighboring light atoms from their equilibrium positions. We tried the following displacement vectors $(D,0,0)$, $(D,D,0)$, and (D,D,D). All other atoms were initially at their lattice positions and all atoms had zero initial velocities. Breather's initial amplitude, D, was taken from the range $0.01a \leq D \leq 0.05a$. After short transient period (about ten periods of breather's oscillations), associated with partial energy radiation in the form of small-amplitude lattice vibrations, spatially localized vibrational mode, i.e., DB, emerged. At the beginning, DB had the form similar to the form of initial excitation. However, we found that DB with polarization [111], produced by the initial condition (D,D,D), was unstable and after a few tens or a hundred of oscillations it abruptly transformed into DB [110] or [100].

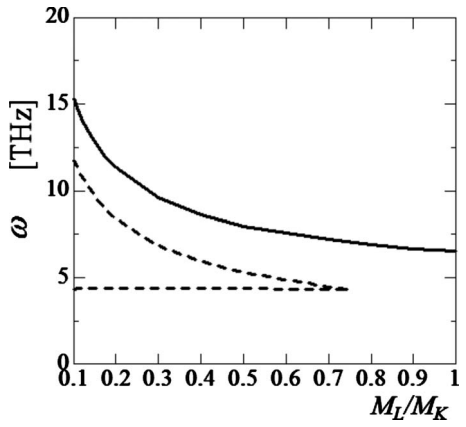

FIG. 3. The maximum frequency (solid line) and edges of the gap (dashed line) of the phonon spectrum, as the functions of the mass ratio of atoms M_L/M_K.

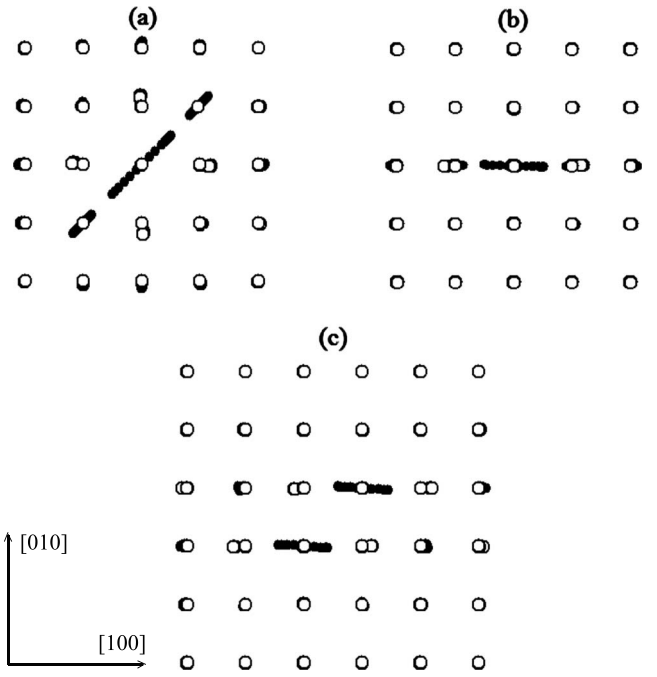

FIG. 4. Stroboscopic pictures showing motion of atoms for the DBs of three types: (a) $[110]_1$, (b) $[100]_1$, and (c) $[100]_2$, where figures in brackets describe polarization and the subscript indicates the number of the atoms oscillating with large amplitude. In all three cases the [001] component of displacement for the atoms oscillating with large amplitude is zero. In panels (a) and (b) displacements of the atoms from their equilibrium positions are multiplied by factor 7, and in panel (c) by factor 5. Heavy (light) atoms are shown by open (filled) circles.

Nevertheless, for exciting a DB, the most efficient initial condition was the displacement vector (D,D,D), in spite of the fact that no stable DB with polarization [111] was found. It was easier to get a stable DB of the type [110] or [100] starting with the displacement vector (D,D,D).

For $M_L/M_K=0.1$ we were able to excite three stable DBs, for which the stroboscopic pictures of atomic motion are presented in Fig. 4. In panels (a) and (b) only one light atom has considerable amplitude of oscillation, and vibrations are in [110] and [100] directions, respectively. In panel (c) one can see that two neighboring light atoms have large amplitudes and oscillations are in the direction of [100]. In the following we will refer to the three types of DBs giving in the brackets their polarization with the subscript indicating the number of atoms oscillating with large amplitude. Note that in all cases DBs are characterized by a high degree of spatial localization of atomic displacements. Degree of spatial localization of DB increases with the decrease in M_L/M_K.

In Fig. 5 we give the DB's frequency ω as the function of its amplitude A. Smooth dashed curves connect the dots obtained in numerical experiments. Horizontal line indicates the upper edge of the phonon gap. Solid line gives $\omega(A)$ found for the DB $[100]_1$ in frame of the single degree of freedom model introduced in Sec. III C. Increase (decrease) in DB's amplitude was carried out by increasing (decreasing) velocity of motion of all atoms by 1% at the moment when

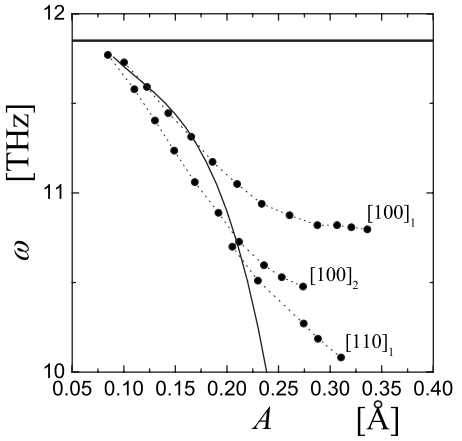

FIG. 5. Frequency as the function of amplitude of the excited atom(s) for the three types of DBs found in our simulations for $M_L/M_K=0.1$. Solid line gives $\omega(A)$ found for the DB $[100]_1$ in frame of the single degree of freedom model introduced in Sec. III C. Horizontal line gives the upper edge of the phonon gap.

the DB's kinetic energy reached its maximum. The energy increase or decrease was followed by the period of stabilization of DB for 50 periods of its oscillations, and then its frequency and amplitude were measured. Frequencies of DBs lie in the gap of the phonon spectrum and, for this reason, DBs practically do not radiate energy over the crystal. Reduction in DBs' frequency with increase in their amplitudes suggests the soft type of nonlinearity in the considered crystal.

It was found that DB $[110]_1$ can have amplitude (in angstroms) in the range $0.2 \leq A \leq 0.31$ while the amplitude of DB $[100]_1$ lies in the range $0.1 \leq A \leq 0.34$ and that of DB $[100]_2$ in the range $0.08 \leq A \leq 0.28$ (see Fig. 5). Attempts to decrease or increase the amplitudes beyond the specified limits led to different results for different DBs.

An attempt to increase the amplitudes of the DB $[110]_1$ or $[100]_2$ beyond the maximal possible values led to their transformation into the DB $[100]_1$. An example of such transformation is shown in Fig. 6 for the case $[100]_2 \rightarrow [100]_1$. Here thin and thick lines show the x components of displacements of two atoms oscillating with large amplitude as the functions of time. One can see from Fig. 6 that, due to the instability of motion with present amplitude, one of the excited atoms of DB $[100]_2$ gives its energy to another excited atom, thus transforming the original DB to the DB of type $[100]_1$.

An attempt to increase the oscillation amplitude of DB $[100]_1$ beyond the upper limit denoted in Fig. 5, led to rapid

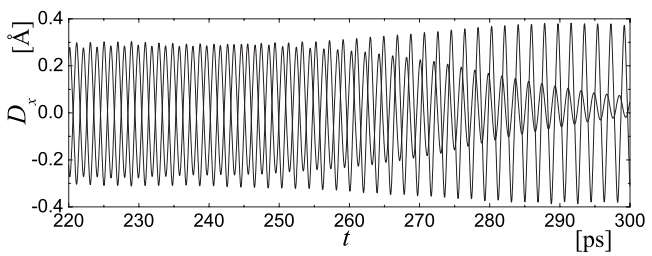

FIG. 6. Example of transformation of DB $[100]_2$ into DB $[100]_1$ after an attempt to increase the amplitude of the original DB above the value of 0.28 Å.

TABLE II. The energy of formation of vacancy pairs in alkali halides (Ref. 23).

Alkali halide	M_L/M_K	E_v, kcal/mol
LiBr	0.09	10.38
		23.98
NaI	0.18	20.76
		26.06
LiCl	0.22	8.99
		25.6
RbF	0.22	21.22
		29.29
NaBr	0.29	20.99
		27.67
KI	0.31	24.68
		27.21

radiation of energy in the form of small-amplitude thermal vibrations over the crystal lattice and decreasing of its amplitude to maximal possible value, $A=0.34$ Å. An attempt to reduce the amplitude of the DB $[110]_1$ below the value 0.2 Å also led to its transformation into the DB $[100]_1$. As to the DB $[100]_1$ and DB $[100]_2$, at small amplitudes their frequencies are close to the upper edge of the gap, therefore they excite phonons, radiate energy and disappear.

Also we found the largest and the smallest values of DB energy, i.e., energy of DB when it has maximal or minimal amplitude of oscillations. The energy of DB $[100]_1$ can vary within the range (in kcal/mol) $0.99 \leq E \leq 5.16$, the energy of DB $[110]_1$ lies in the range $4.67 \leq E \leq 5.15$, and for the DB $[100]_2$ it is in the range $1.65 \leq E \leq 6.86$. As one can see, DB's energy is comparable to the energy of formation of vacancy pairs in alkali halide crystals, see some of the results of work[23] in Table II. For each salt the energy of vacancy pairs calculated with the general relaxation are given by two rows, the first one gives the value obtained with the Born-Mayer potential and the second row with the Born-Mayer-Verwey potential.[23]

For the mass ratio of $M_L/M_K=0.18$ (as for NaI) we were able to excite only one type of DB, namely, $[100]_1$. In Fig. 7 we plot the DB frequency as the function of its amplitude in this case.

For the mass ratio of $M_L/M_K=0.2$ we were unable to excite any DB. We also tried to obtain a DB for this value of the atomic mass ratio starting from the stable DB at $M_L/M_K=0.18$ and slowly increasing the mass of the light component. The rate of change in atomic mass was so small that within one period of DB oscillation it was practically unchanged. Nevertheless, on approaching the mass ratio $M_L/M_K=0.2$ the lifetime of DB became rather short (less than a hundred of oscillations). We thus conclude that for the interatomic potentials used in our study DB can exist only for $M_L/M_K<0.2$. An explanation of this fact will be offered in Sec. III C.

C. Single degree of freedom model

We have made an attempt to describe DB dynamics by a single degree of freedom model. Let us consider DB $[100]_1$

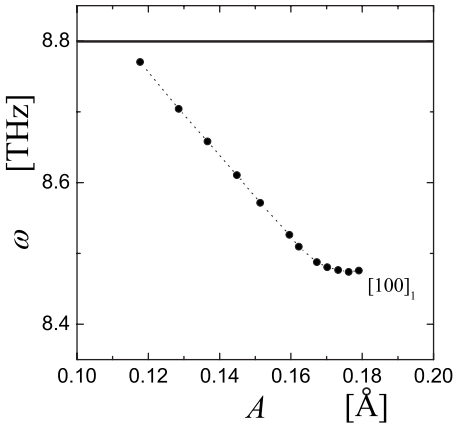

FIG. 7. Frequency of DB $[100]_1$ as the function of its amplitude for the mass ratio $M_L/M_K=0.18$.

and denote the displacement of the atom moving with large amplitude from its lattice position by ξ. We need to know the potential energy landscape $U(\xi)$ where the atom oscillates. This can be found under assumption that total energy of the atom is conserved, then one can write $U(\xi)=-P[\xi(t)]$, where P is the kinetic energy of the atom. In Fig. 8, by black solid lines we show $U(\xi)$ for ten periods of DB as found from MD simulations. Eight curves correspond to DBs with different oscillation amplitudes $A=\xi_{\max}$. Dashed lines are the fits of the curves $U(\xi)$ by the functions

$$U(\xi) = a\xi^2 + b\xi^4. \tag{2}$$

The fitting curves are in a good agreement with the MD results for not very large A (<0.2 Å).

Equation of motion of the atom of mass M_L in this potential is

$$\ddot{\xi} + \alpha\xi + \beta\xi^3 = 0, \tag{3}$$

where

$$\alpha = \frac{2a}{M_L}, \quad \beta = \frac{4b}{M_L}. \tag{4}$$

Approximate solution to Eq. (3) can be written as

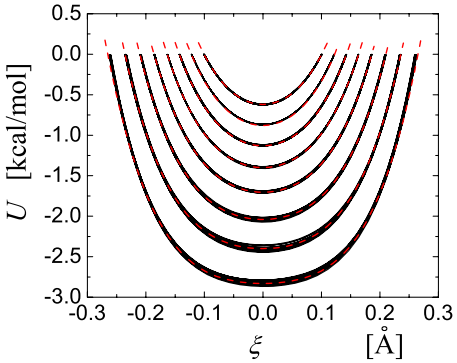

FIG. 8. (Color online) $U(\xi)$ for DBs $[100]_1$ with different amplitudes $A=\xi_{\max}$ as found from MD simulations for ten periods of oscillation (black solid lines) and fitting curves Eq. (2) (dashed lines). Results for $M_L/M_K=0.1$.

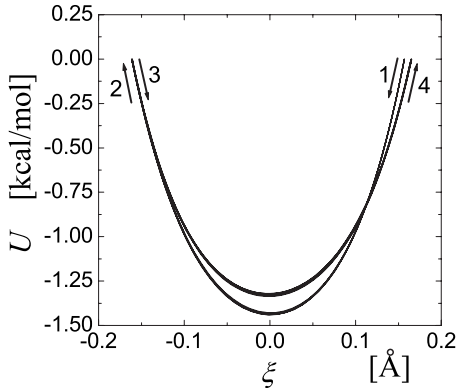

FIG. 9. $U(\xi)$ for a DB $[100]_1$ as found from MD simulations for ten periods of oscillation. Result for $M_L/M_K=0.18$.

$$\xi(t) = A\,\sin(\omega t) + A_1\,\sin(3\omega t),$$

$$\omega^2 = \alpha + \frac{3}{4}\beta A^2,$$

$$A_1 = \frac{-\beta A^3}{32\alpha + 27\beta A^2}, \tag{5}$$

where it is assumed that $A \ll 1$ and $A_1 \ll A$.

For the set of fitting curves shown in Fig. 8 we have found that the parameters a and b of the potential Eq. (2) depend on the DB amplitude A linearly

$$a(A) = R_a A + S_a, \quad b(A) = R_b A + S_b \tag{6}$$

with $R_a=-258.7$ kcal/(mol Å^3), $S_a=77.76$ kcal/(mol Å^2), $R_b=1205$ kcal/(mol Å^5), and $S_b=-3501$ kcal/(mol Å^4).

Now one can calculate the frequency of the atom in the effective potential as the function of its amplitude A. To do so, for chosen A, we first find a, b from Eq. (6), then α, β from Eq. (4), and finally ω from the second expression in Eq. (5). The result is presented in Fig. 5 by solid line. This curve gives a good approximation of the corresponding curve for the DB $[100]_1$ for $A<0.2$ Å. For larger A the deviation increases because the decrease in the "exact" dashed curve slows down with increasing A. This can be explained by the influence of the higher order anharmonic terms that were neglected in the approximation of $U(\xi)$ expressed by Eq. (2).

It is important to note that the anharmonic coefficient b is *positive* in the whole range of DB's amplitude A, as it follows from the approximation Eq. (6). It is well known that positive b (and thus, positive β) corresponds to rigid type of nonlinearity with frequency of atom *increasing* with A. Thus, the decrease in the frequency observed in our case is due to the fact that α and β are the functions of A. Coefficients α and β change with A because the atom oscillating with large amplitude shifts positions of neighboring atoms.

Let us turn to the case of mass ratio $M_L/M_K=0.18$. In Fig. 9 we show $U(\xi)$ for ten periods of DB as found from MD simulations for the DB $[100]_1$. A remarkable difference of this result from that presented in Fig. 8 for $M_L/M_K=0.1$ is that when the central atom moves in positive direction it experiences potential different from that when it moves in

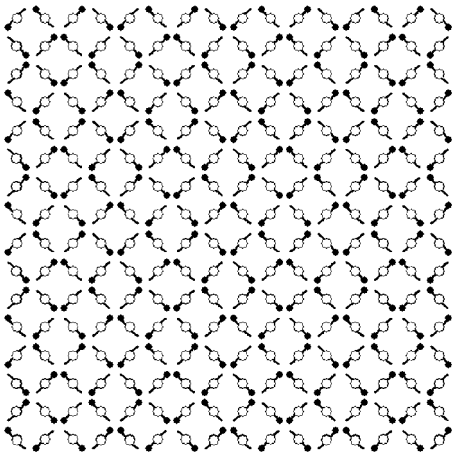

FIG. 10. Example of the zone-boundary phonon mode (x,y projection) for $B=0.02$ Å. Displacements of atoms are multiplied by factor 50. Heavy atoms are shown by open circles, trajectories of the light atoms by dots, and initial positions of the light atoms by large dots.

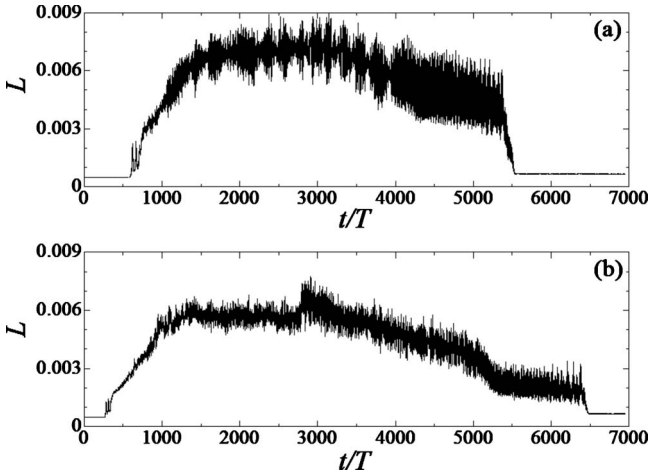

FIG. 11. Time evolution of the localization parameter L for the initial amplitude of the phonon zone-boundary mode (a) $B=0.02$ Å and (b) $B=0.03$ Å. Here $M_L/M_K=0.1$ and T is the period of DB oscillation.

the opposite direction. This dependence of the potential on the direction of motion of the central atom appears because the neighboring atoms have oscillation harmonic with the frequency equal to half of the main frequency of the central atom. Presence of the harmonic with frequency equal to half of the main frequency explains the short lifetime of DBs observed for $M_L/M_K=0.2$. For this mass ratio, frequency of the upper edge of the phonon gap is equal to doubled frequency of the lower edge, as it can be seen in Fig. 3. The vibrational mode with the frequency equal to half of the main DB frequency interacts with the phonons below the gap when $M_L/M_K \geq 0.2$.

D. Anti-FPU mechanism of DBs excitation

The zone-boundary phonon mode, with only light atoms moving, was excited in the crystal as follows: two of the light atoms in each translational cell of the crystal, located in different [100] planes, were initially displaced by the vector (B,B,B) and the other two by the vector $(-B,-B,-B)$. Heavy atoms were at their lattice positions and initial velocities of all atoms were equal to zero. For the mode amplitude, B, we considered two values, $B=0.02,0.03$ Å. Computational cell in this simulation included $8\times8\times8$ translational cells. Example of the excited mode (x,y projection) for $B=0.02$ Å, is shown in Fig. 10 with the displacements of atoms multiplied by factor 50. Heavy atoms are shown by open circles, trajectories of the light atoms by dots and the initial positions of the light atoms by large dots.

The zone-boundary modes with $B=0.02$ and 0.03 Å, were found to be unstable. Evolution of the unstable mode led to spatial energy localization in the form of DBs. In order to characterize the degree of energy localization in the crystal we calculated the localization parameter

$$L=\frac{\sum_{n=1}^{N}E_n^2}{\left(\sum_{n=1}^{N}E_n\right)^2}, \tag{7}$$

where E_n is the averaged over period of DB total energy of the nth light atom and summation is over all light atoms in the computational cell (heavy atoms were not taken into account in the calculation of L).

In Fig. 11, for the case of $M_L/M_K=0.1$, we give L as the function of dimensionless time t/T, where T is the period of DB. Results are given for the initial amplitude of the phonon zone-boundary mode (a) $B=0.02$ Å and (b) $B=0.03$ Å. Before the modulational instability breaks the phonon mode, the localization parameter is equal to its smallest possible value of $L=1/N$. Then L starts to increase rapidly due to the energy localization in the form of large-amplitude DBs. Then L reaches its maximal value that remains almost unchanged for about 5000 breather oscillations. During this period DBs gradually radiate their energy. Eventually DBs disappear and L drops to the value on order of $1/N$ and remains small forever since the system reaches its thermal equilibrium.

In Fig. 12, one can see two large-amplitude DBs formed at $t=1000T$ as the result of evolution of the modulationally unstable zone-boundary phonon mode presented in Fig. 10. Displacements of atoms are multiplied by factor 10.

In Fig. 13 we present E_n ordered by decrease for the case of $M_L/M_K=0.1$ and for the initial amplitudes of the phonon zone-boundary mode (a) $B=0.02$ Å and (b) $B=0.03$ Å. Dots show the results for the time $t/T=1000$ and circles for the time $t/T=3000$. Atoms with large energies E_n correspond to DBs. One can see that in case (a) four while in case (b) five DBs emerged.

IV. CONCLUSIONS

The results of molecular-dynamics simulations of DBs in the crystals with NaCl structure with different ratios of

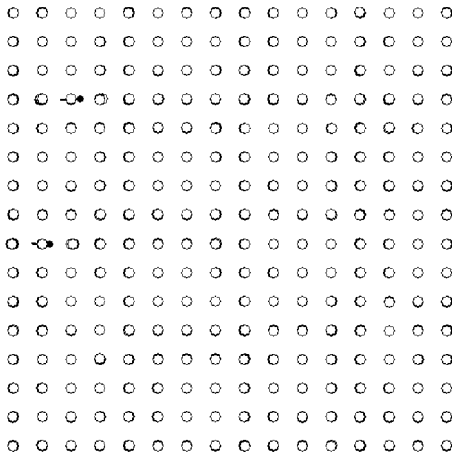

FIG. 12. Two large-amplitude DBs formed as the result of evolution of the modulationally unstable zone-boundary phonon mode presented in Fig. 10. Displacements of atoms are multiplied by factor 10.

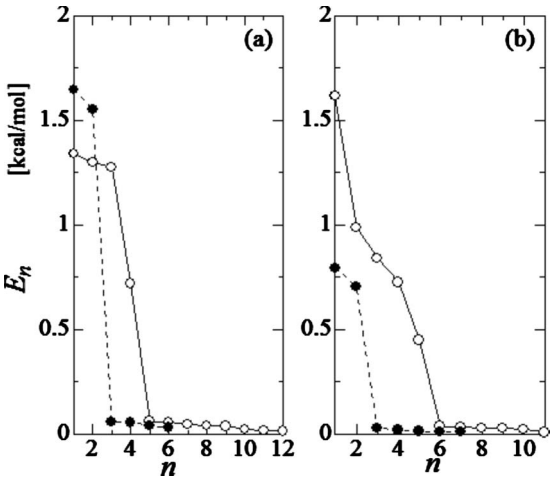

FIG. 13. Total energies of the light atoms averaged over one period of DB oscillation, E_n, ordered by decrease, for the initial amplitude of the phonon zone-boundary mode (a) $B=0.02$ Å and (b) $B=0.03$ Å. Dots show the results for the time $t/T=1000$ and circles for the time $t/T=3000$, where T is the period of DB oscillation. Here $M_L/M_K=0.1$.

atomic masses of components, presented in this paper, can be summarized as follows. (1) In the crystal with the atomic weight ratio $M_L/M_K=0.1$ we were able to excite three different types of stable DBs, namely, $[100]_1$, $[110]_1$, and $[100]_2$, where figures in the brackets describe the polarization of atomic oscillations and the subscript index specifies the number of atoms with large amplitude (see Fig. 4). In our simulations DBs with polarization [111] were found to be unstable and after a few tens or a hundred of oscillations they transformed into DBs $[100]_1$ or $[110]_1$. Note that the DBs reported in Refs. 6 and 7 had polarization [111]. Such a difference can be explained by the fact that we used interatomic potentials somewhat different from that used in Ref. 7. (2) In crystals with long-range Coulomb interaction, considered in Ref. 7 and in the present study, DBs demonstrate a soft type of anharmonicity because their frequency decreases with increase in their amplitude (see Figs. 5 and 7). The same was observed for the diatomic crystals with Morse interatomic potentials.[10,12] (3) For $M_L/M_K=0.18$ only one type of DB exists and for $M_L/M_K>0.2$ we could not obtain a stable DB. Thus, for the potentials used in our study, DB can be excited only for $M_L/M_K<0.2$, while, as it can be seen from Fig. 3, the gap in the phonon band is still rather wide at $M_L/M_K=0.2$. Nonexistence of DBs for the mass ratios larger than 0.2 is explained through the excitation of the harmonic with the frequency equal to half of the main DB frequency that interacts with phonons below the gap (see Sec. III C, Fig. 9). (4) The most stable DB among found was DB $[100]_1$, i.e., DB with one excited atom, oscillating in the direction [100], as shown in Fig. 4(a). DBs $[110]_1$ and $[100]_2$, when we tried to increase their amplitudes beyond certain critical values, became unstable and transformed into the DB $[100]_1$. (5) Single degree of freedom model gives a good approximation of the dependence of DB frequency vs amplitude for $A<0.2$ Å, see Sec. III C. (6) DBs can have very high energies, comparable to the energy of vacancy pairs in alkali halides, see Table II.[23] The energies of DBs found in this work lie in the following ranges (in kcal/mol): DB $[100]_1$ in the range $0.99\leq E\leq 5.16$, DB $[110]_1$ in the range $4.67\leq E\leq 5.15$, and DB $[100]_2$ in the range $1.65\leq E\leq 6.86$. (7) The anti-FPU mechanism of energy localization[18] does work for the crystals with NaCl structure with interatomic potentials used in the present study, see Sec. III D.

As the open problems for future studies we would like to propose the following: (i) influence of temperature on the life time of DB; (ii) search for DBs in thermal equilibrium; and (iii) search for the materials with hard anharmonicity supporting DBs with frequencies above the phonon band.

ACKNOWLEDGMENTS

The authors gratefully acknowledge the financial support provided by the Russian Foundation for Basic Research under Grant No. 09-08-00695-a.

[1] A. J. Sievers and S. Takeno, Phys. Rev. Lett. **61**, 970 (1988).
[2] S. Flach and C. R. Willis, Phys. Rep. **295**, 181 (1998).
[3] S. Flach and A. V. Gorbach, Phys. Rep. **467**, 1 (2008).
[4] D. K. Campbell, S. Flach, and Yu. S. Kivshar, Phys. Today **57**(1), 43 (2004).
[5] Yu. S. Kivshar and G. P. Agrawal, *Optical Solitons: From Fibers to Photonic Crystals* (Academic, New York, 2003).
[6] M. E. Manley, A. J. Sievers, J. W. Lynn, S. A. Kiselev, N. I. Agladze, Y. Chen, A. Llobet, and A. Alatas, Phys. Rev. B **79**, 134304 (2009).

[7] S. A. Kiselev and A. J. Sievers, Phys. Rev. B **55**, 5755 (1997).
[8] A. R. Bishop, A. Bussmann-Holder, S. Kamba, and M. Maglione, Phys. Rev. B **81**, 064106 (2010).
[9] A. V. Savin and Y. S. Kivshar, EPL **89**, 46001 (2010).
[10] S. V. Dmitriev, A. A. Sukhorukov, A. I. Pshenichnyuk, L. Z. Khadeeva, A. M. Iskandarov, and Yu. S. Kivshar, Phys. Rev. B **80**, 094302 (2009).
[11] S. V. Dmitriev, N. N. Medvedev, R. R. Mulyukov, O. V. Pozhidaeva, A. I. Potekaev, and M. D. Starostenkov, Russ. Phys. J. **51**, 858 (2008).
[12] S. V. Dmitriev, L. Z. Khadeeva, A. I. Pshenichnyuk, and N. N. Medvedev, Phys. Solid State **52**, 1499 (2010).
[13] V. Dubinko, Nucl. Instrum. Methods Phys. Res. B **267**, 2976 (2009).
[14] M. E. Manley, arXiv:0905.2988 (unpublished).
[15] M. E. Manley, Acta Mater. **58**, 2926 (2010).
[16] T. Shimada, D. Shirasaki, and T. Kitamura, Phys. Rev. B **81**, 035401 (2010).
[17] Y. Kinoshita, Y. Yamayose, Y. Doi, A. Nakatani, and T. Kitamura, Phys. Rev. B **77**, 024307 (2008).
[18] T. Dauxois, R. Khomeriki, F. Piazza, and S. Ruffo, Chaos **15**, 015110 (2005).
[19] A. V. Gorbach and M. Johansson, Phys. Rev. E **67**, 066608 (2003).
[20] G. James and M. Kastner, Nonlinearity **20**, 631 (2007).
[21] S. Tsuneyuki, H. Aoki, M. Tsukada, and Y. Matsui, Phys. Rev. Lett. **64**, 776 (1990).
[22] S. V. Dmitriev, D. A. Semagin, T. Shigenari, K. Abe, M. Nagamine, and T. A. Aslanyan, Phys. Rev. B **68**, 052101 (2003).
[23] K. Tharmalingam, J. Phys. C **3**, 1856 (1970).